

Energy spectra of small bosonic clusters having a large two-body scattering length

M. Gattobigio,¹ A. Kievsky,² and M. Viviani²

¹*Université de Nice-Sophia Antipolis, Institut Non-Linéaire de Nice, CNRS, 1361 route des Lucioles, 06560 Valbonne, France*

²*Istituto Nazionale di Fisica Nucleare, Largo Pontecorvo 3, 56100 Pisa, Italy*

(Received 5 June 2012; published 26 October 2012)

In this work we investigate small clusters of bosons using the hyperspherical harmonic basis. We consider systems with $A = 2, 3, 4, 5, 6$ particles interacting through a soft interparticle potential. In order to make contact with a real system, we use an attractive Gaussian potential that reproduces the values of the dimer binding energy and the atom-atom scattering length obtained with one of the most widely used ^4He - ^4He interactions, the LM2M2 potential of Aziz and Slaman. The intensity of the potential is varied in order to explore the clusters' spectra in different regions with large positive and large negative values of the two-body scattering length. In addition, we include a repulsive three-body force to reproduce the trimer binding energy. With this model, consisting in the sum of a two- and three-body potential, we have calculated the spectrum of the four-, five-, and six-particle systems. In all the regions explored, we have found that these systems present two states, one deep and one shallow close to the $A - 1$ threshold. Some universal relations between the energy levels are extracted; in particular, we have estimated the universal ratios between thresholds of the three-, four-, and five-particle continua using the two-body Gaussian potential. They agree with recent measurements and theoretical predictions.

DOI: [10.1103/PhysRevA.86.042513](https://doi.org/10.1103/PhysRevA.86.042513)

PACS number(s): 31.15.ac

I. INTRODUCTION

Systems composed by few atoms having large value of the two-body scattering length a with respect to the natural length ℓ fixed by the atomic potential have been the object of an intense investigation both from a theoretical and an experimental point of view (for recent reviews, see Refs. [1–3]). In fact, they present universal properties: for example, the three-body system displays the Efimov effect [4,5], which means the appearance, in the limit $a/\ell \rightarrow \infty$, of an infinite set of bound states accumulating toward the three-particle threshold; moreover, the three-body spectrum has a discrete-scale symmetry, with a universal ratio between the n th and $(n + 1)$ th levels $E_3^{n+1}/E_3^n = e^{-2\pi/s_0}$. The scaling factor depends only on the ratio between particle masses, and for identical bosons of mass m it reads as $e^{-2\pi/s_0} \approx 1/515.03$ (with $s_0 \approx 1.00624$). The finite value of ℓ implies the existence of a three-body ground state E_3^0 , the value of which reflects the short-range physics, and that, together with the discrete-scale symmetry, completely determines the spectrum. In realistic cases, the ratio a/ℓ is large but finite; thus, the three-body spectrum reduces to a finite number of states.

A remarkable property in the $a \rightarrow \infty$ limit appears in the four-body system: two states $E_4^{n,0}, E_4^{n,1}$ are attached to each trimer state E_3^n , one deep and one shallow having universal ratios $E_4^{n,0}/E_3^n \approx 4.6$ and $E_4^{n,1}/E_3^n \approx 1.001$ [6–8]; the two lowest four-body states, $E_4^0 = E_4^{0,0}$ and $E_4^1 = E_4^{0,1}$, are real bound states. These properties have been studied for large positive and large negative values of the scattering length in the (a^{-1}, κ) plane, with $\kappa = \text{sign}(E)[|E|/(\hbar^2/m)]^{1/2}$, constructing what is normally called an Efimov plot [9].

There are very few studies of the spectrum of small bosonic clusters beyond $A = 4$. In addition to the specific problems related to the solution of the Schrödinger equation for more than four particles, the atom-atom realistic potentials present a strong repulsion at short distances, which makes the numerical problem more difficult. Specific algorithms

have been developed so far to solve this problem: the Faddeev equation has been opportunely modified [10], the hyperspherical methods resorted either to the hyperspherical adiabatic (HA) expansion (for a review, see Ref. [11]) or to the correlated hyperspherical harmonic expansion (CHH) [12]. However, due to the difficulties in treating the strong repulsion, few calculations exist for systems with more than three atoms. For example, in Ref. [13] the diffusion Monte Carlo method has been used to describe the ground state of ^4He molecules up to 10 atoms, and in Ref. [14] a very extended calculation has been done in the four-helium-atom system. On the other hand, descriptions of few-bosons systems using soft-core potentials are currently operated (see, for example, Refs. [7,15]).

The equivalence between hard- or soft-core-potential descriptions has been discussed in Refs. [16,17], in which an attractive soft ^4He - ^4He Gaussian potential has been used to investigate the three-atom system. The soft-two-body potential was designed to reproduce the helium dimer binding energy E_2 , the ^4He - ^4He scattering length a , and the effective range r_0 of the LM2M2 potential [18], one of the most used ^4He - ^4He interactions. In this context, the soft Gaussian potential can be considered as a regularized-two-body contact term in an effective field theory (EFT) approximation of the LM2M2 [19]; this is possible because of the scale separation between the ^4He - ^4He scattering length $a = 189.41$ a.u., and the natural length $\ell = 10.2$ a.u., which is the van der Waals length calculated for the LM2M2 potential [1].

In the two-body sector and in the low-energy limit, the two potentials predict similar phase shifts, therefore, even if their shape is completely different, they describe in an equivalent way the physical processes in that limit [19]. The equivalence is lost as the energy is increased, when the details of the potential become more and more important. When the soft interaction is used in the three-body sector, a new three-body contact term is required to reproduce the ground-state binding energy of the helium trimer given by the LM2M2 potential. This term is introduced by means of a Gaussian-hypercentral three-body

force, the strength of which is tuned to reproduce the LM2M2 ground-state binding energy of the three-atom system. In Ref. [16], the quality of this description has been studied for different ranges of the three-body force by comparing the binding energy of the excited Efimov state and the low-energy helium-dimer phase shifts to those obtained with the LM2M2 potential. In Ref. [17], the spectrum of small clusters of helium atoms has been investigated up to six particles maintaining, however, fixed the values of a and E_2 as given by the LM2M2 potential.

In this work we extend the analysis of the $A = 3 - 6$ bosonic spectrum to the (a^{-1}, κ) plane. We have modified the strength of the LM2M2 potential in order to cover the region of negative values of a up to a_-^0 , with this value indicating the threshold of having a three-body system bound. We have also increased the intensity of the interaction in order to extend the analysis to positive values of a in which the universal character of the system starts to be questionable, i.e., when the ground-state E_3^0 approaches the natural energy $E_\ell = -\hbar^2/m\ell^2$, which delimits the Efimov window.

Associated with the different values of a of the modified LM2M2 potential, we have constructed a set of attractive Gaussian potentials with the strength fixed to reproduce the low-energy data of LM2M2. Moreover, the modifications of the LM2M2 produce different values of the $A = 3$ ground-state energy E_3^0 ; accordingly, we introduce a soft three-body force devised to reproduce those values along the (a^{-1}, κ) plane. Within this model, consisting in the sum of a two- and a three-body potential, we have calculated the spectrum of the four-, five-, and six-particle systems.

Two different calculations have been performed in this work. From one side, we have calculated the $A = 3$ ground state and excited states E_3^0 and E_3^1 , using the LM2M2 potential and its modification, in order to construct the corresponding Efimov plot. Since this potential presents a strong short-range repulsion, we have used the CHH expansion as discussed in Ref. [12]. On the other side, when using the soft-core-potential model in systems with $A \geq 3$, the numerical calculations were performed by means of the nonsymmetrized hyperspherical harmonic (NSHH) expansion method with the technique recently developed by the authors in Refs. [17,20–22]. In this approach, the authors have used the hyperspherical harmonic (HH) basis, without a previous symmetrization procedure, to describe bound states in systems up to six particles. The method is based on a particular representation of the Hamiltonian matrix, as a sum of products of sparse matrices, well suited for a numerical implementation. Converged results for different eigenvalues, with the corresponding eigenvectors belonging to different symmetries, have been obtained [22]. In this work, since we are dealing with bosons, we only consider the symmetric part of the spectrum. Interestingly, we have observed that in all the regions explored, the $A = 4, 5, 6$ systems present two states, one deep and one shallow close to the E_{A-1}^0 threshold. To gain insight on the shallow state, for a selected value of a , we have varied the range of the three-body force and we have studied the effect of that variation in the $A = 4, 5, 6$ spectrum. In the range considered, the variation produces small changes in the eigenvalues, but they are crucial to determine if the shallow state is bound or not with respect to the $A - 1$ threshold. This

analysis confirms, at least in one zone of the Efimov plot, previous observations that each Efimov state in the $A = 3$ system produces two bound states in the $A = 4$ system, and extends this observation to the $A = 5, 6$ systems.

Finally, we have extended the calculations of the $A = 4$ and 5 systems up to the four- and five-particle thresholds using the simple two-body Gaussian potential; the ratios between the thresholds are in agreement with previous theoretical results [7,23] and with experiments [24–27].

The paper is organized as follows. In Sec. II, we describe the two- and three-body forces we used in our calculations to reproduce the LM2M2 values. In Sec. III, we discuss the Efimov plot for three particles. In Sec. IV, the results for the bound states of the $A = 3, 4, 5, 6$ clusters are discussed, whereas the conclusions are given in the last section.

II. SOFT-CORE TWO- AND THREE-BODY POTENTIALS

As mentioned in the Introduction, we use the LM2M2 $^4\text{He}-^4\text{He}$ potential as the reference interaction, with the mass parameter fixed to $\hbar^2/m = 43.281\,307(\text{a.u.})^2 \text{K}$. In order to explore the Efimov (a^{-1}, κ) plane, we have modified the LM2M2 interaction as follows:

$$V_\lambda(r) = \lambda V_{\text{LM2M2}}(r). \quad (1)$$

Examples of this strategy exist in the literature [12,28]. We have varied λ from $\lambda = 0.883$, where $a = a_-^0 = -43.84 \text{ a.u.}$, up to $\lambda = 1.1$ corresponding to $a = 44.79 \text{ a.u.}$, as shown in Fig. 1. The unitary limit is produced for $\lambda \approx 0.9743$. When $\lambda = 1$, the values of the LM2M2 are recovered: $a = 189.41 \text{ a.u.}$, $E_2 = -1.303 \text{ mK}$, and $r_0 = 13.845 \text{ a.u.}$

Following Refs. [11,16,17], we have constructed an attractive two-body Gaussian (TBG) potential

$$V(r) = V_0 e^{-r^2/R_0^2}, \quad (2)$$

with range $R_0 = 10 \text{ a.u.}$, and we have varied the strength V_0 in order to reproduce the values of a given by $V_\lambda(r)$, as shown in Fig. 2. For $\lambda = 1$ with the strength $V_0 = -1.234\,356\,6 \text{ K}$, we

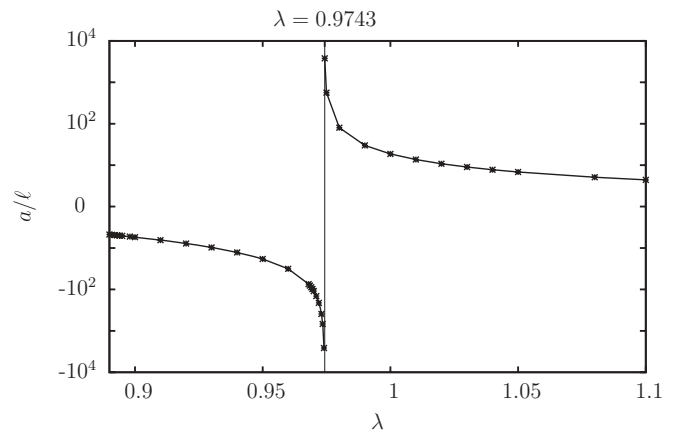


FIG. 1. The scattering length a , in units of ℓ , as a function of the parameter λ , calculated with the modified LM2M2 potential $V_\lambda(r)$. The range of variation of λ is between $\lambda = 0.883$, which corresponds to the disappearance in the continuum of the excited three-body state, and $\lambda = 1.1$. The unitary limit is obtained for $\lambda \approx 0.9743$.

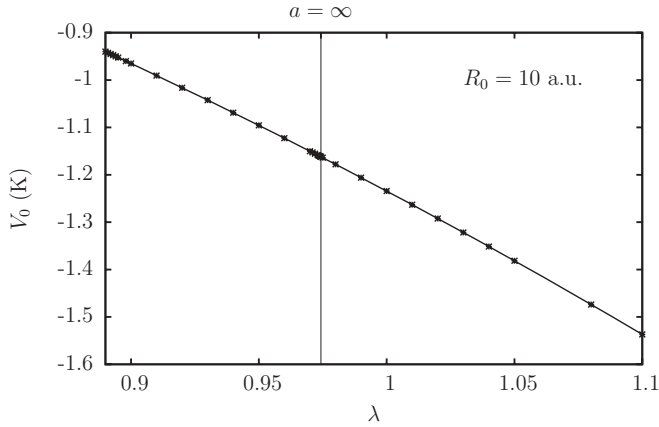


FIG. 2. The strength V_0 of the Gaussian two-body potential as a function of the parameter λ . The values are tuned to reproduce the scattering length a given by the modified LM2M2 potential $V_\lambda(r)$.

reproduce the LM2M2 low-energy data, $E_2 = -1.303$ mK, $a = 189.42$ a.u., and $r_0 = 13.80$ a.u. The use of the TBG potential in the three-atom system produces a ground-state binding energy appreciably deeper than the one calculated with $V_\lambda(r)$. For example, at $\lambda = 1$, the LM2M2 helium trimer ground-state binding energy is 126.4 mK, whereas the one obtained using the two-body soft-core potential in Eq. (2) is 151.32 mK. A smaller difference, although still appreciable, can be observed in the first excited state.

In order to have a closer description to the $A = 3$ system obtained with the modified LM2M2 potential, we introduce the following (repulsive) hypercentral-three-body (H3B) interaction

$$W(\rho_{123}) = W_0 e^{-\rho_{123}^2/\rho_0^2}, \quad (3)$$

with the strength W_0 tuned to reproduce the trimer energy E_3^0 obtained using $V_\lambda(r)$ for all the explored values of λ , as shown in Fig. 3. Here, $\rho_{123}^2 = \frac{2}{3}(r_{12}^2 + r_{23}^2 + r_{31}^2)$ is the hyperradius of three particles and ρ_0 gives the range of the three-body force or, in the spirit of EFT, the cutoff of the three-body contact interaction; therefore, it is not independent of R_0 , which is the

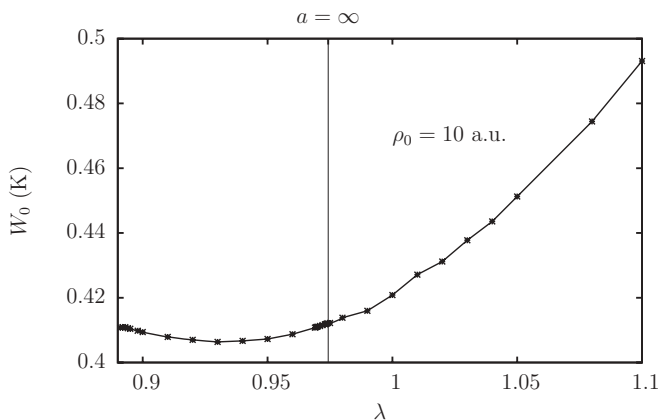


FIG. 3. The strength W_0 of the hypercentral three-body potential as a function of the parameter λ . The values are tuned to reproduce the three-body ground state E_3^0 given by the modified LM2M2 potential $V_\lambda(r)$.

cutoff of the two-body contact force, and in fact it should be $\rho_0 = R_0$, as shown in Ref. [17], and so we fixed $\rho_0 = 10.0$ a.u. A different criterion to fix the three-body force was given in Ref. [23] in which the condition $\rho_0 \gg r_0$ has been used. In this case, the (repulsive) three-body force is used to push the trimer spectrum high in energy in order to verify as close as possible the universal ratios $E_3^{n+1}/E_3^n = e^{-2\pi/s_0}$ already at $n = 0$. With the LM2M2 interaction, this relation is only approximately verified; for $\lambda = 1$, we have $E_3^0/E_3^1 \approx 56$, whereas at the unitary limit $E_3^0/E_3^1 \approx 525$, very close to the universal ratio.

III. THREE-BODY EFIMOV PLOT

The calculations for $A = 3$ have been performed using the CHH expansion. Since $V_\lambda(r)$ is obtained multiplying the LM2M2 potential by a global factor λ , it inherits the strong short-range repulsion; in this case, a direct use of the HH basis to compute the bound states is not feasible since it would be necessary to include an enormous number of basis elements in the expansion [29]. The use of the CHH expansion circumvents this problem by the introduction of a correlation factor of the Jastrow type. The method is described in Ref. [12] and it allows us to achieve similar accuracy as other techniques. As an example, in Table I we show the results for the ground state E_3^0 and the excited state E_3^1 at $\lambda = 1$ (in this case, the results of the LM2M2 potential are recovered), and at the unitary limit $\lambda = 0.9743$. These results have been obtained using the CHH basis up to a value of the grand angular momentum $K = 160$.

As a by-product of the tuning procedure of the three-body strength W_0 , we have constructed, as was previously done for instance in Refs. [28,30], the Efimov plot shown in Fig. 4. In the figure, we report calculations of E_3^0 and E_3^1 as functions of a done both with the $V_\lambda(r)$ and the TBG potential. When the TBG + H3B potential is used, the results coincide with those of $V_\lambda(r)$ and are not reported in the figure. In addition, we draw the dimer energy E_2 , calculated using the $V_\lambda(r)$ potential. In order to show these quantities together, in the figure we have used the fourth root of the energy (in units of E_ℓ) as a function of the square root of a^{-1} (in units of ℓ). In the region analyzed, the results are inside the Efimov window; in fact, the scattering length is still much larger than the natural length ℓ , and the ground-state energy E_3^0 is above the natural value E_ℓ .

TABLE I. The ground state E_3^0 and the excited state E_3^1 of the three-boson system calculated with the modified LM2M2 potential $V_\lambda(r)$, the TBG potential, and the TBG potential plus the H3B potential at $\lambda = 1$, which corresponds to the original LM2M2 potential, and in the unitary limit $\lambda = 0.9743$.

Potential	E_3^0 (mK)	E_3^1 (mK)
$\lambda = 1$		
$V_\lambda(r)$	-126.4	-2.27
TBG	-151.3	-2.48
TBG + H3B	-126.4	-2.31
$\lambda = 0.9743$		
$V_\lambda(r)$	-83.99	-0.16
TBG	-103.4	-0.20
TBG + H3B	-83.99	-0.16

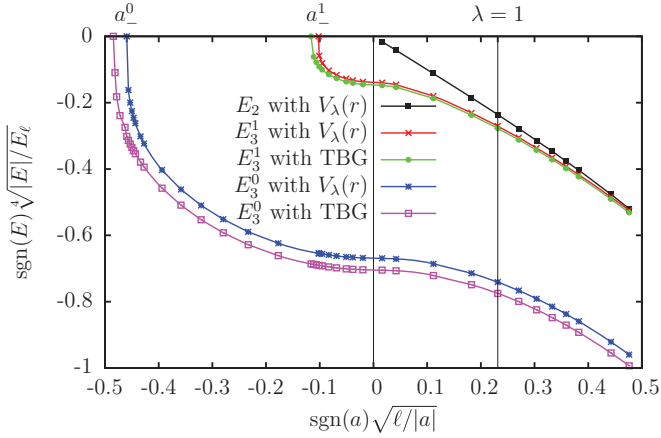


FIG. 4. (Color online) Efimov plot for $A = 3$. We report the ground- and excited-state energies E_3^0 and E_3^1 in units of E_ℓ , as a function of ℓ/a , both for the modified LM2M2 potential $V_\lambda(r)$ and for the TBG potential. Following the literature, we really draw the fourth root of the scaled energies as a function of the square root of the scaled-inverse scattering length; using this trick, the ratio between excited and ground energies is greatly reduced, allowing for the graphical representation of both curves on the same scale. We also report the $A = 2$ binding energy.

Looking in Fig. 4 at negative values of a , it is possible to identify the value of the scattering length a_-^1 at which the excited state E_3^1 disappears. For $V_\lambda(r)$, this value is $a_-^1 \approx -975$ a.u., whereas using the TBG potential it results $a_-^1 \approx -752$ a.u. The next interesting point appears at a_-^0 , when the three-body cluster is no more bound, so that E_3^0 approaches zero. Using $V_\lambda(r)$ this happens at $a_-^0 \approx -48.1$ a.u., whereas using the TBG potential alone it is $a_-^0 \approx -43.3$ a.u.

The ratio a_-^0/a_-^1 has been predicted to have a universal value $(a_-^0/a_-^1)_{\text{theory}} = 22.7$ [1]; in the only experiment which measures the two thresholds (Ref. [24]), the ratio is $(a_-^0/a_-^1)_{\text{experiment}} = 21.1$. In our case, we obtain $(a_-^0/a_-^1)_{\text{TBG}} = 17.4$, and $(a_-^0/a_-^1)_{V_\lambda(r)} = 20.3$, which is closer to both theoretical and experimental values. The absolute position of a_-^0 is not predicted by the theory of Efimov physics and, in that sense, it can be considered as not a universal quantity; however, it has been the subject of experimental measurements which give more or less the same value in units of mean scattering length $\bar{a} = 0.955978 \ell/2$ for different atoms $a_-^0 = -(9 \pm 1) \bar{a}$ [31]. In the present calculations, we obtain $(a_-^0)_{\text{TBG}} = -8.9 \bar{a}$ and $(a_-^0)_{V_\lambda(r)} = -9.9 \bar{a}$.

In addition, we discuss the universal character of the shallow state E_3^1 . Using Efimov's radial law [5], it is possible to obtain an equation for this trimer binding energy as a function of a . It reads as

$$E_3^1 + \frac{\hbar^2}{ma^2} = \exp[\Delta(\xi)/s_0] \frac{\hbar^2 \kappa_*^2}{m}, \quad (4)$$

where κ_* is the wave number corresponding to the energy $E_3^1 = \hbar^2 \kappa_*^2/m = 0.156$ mK at the resonant limit and $\tan \xi = -(mE_3^1/\hbar^2)^{1/2}a$. The function $\Delta(\xi)$ is universal and a parametrization in the range $[-\pi, -\pi/4]$ is given in Ref. [1]. It verifies $\Delta(-\pi/2) = 0$ and, from the very precise result

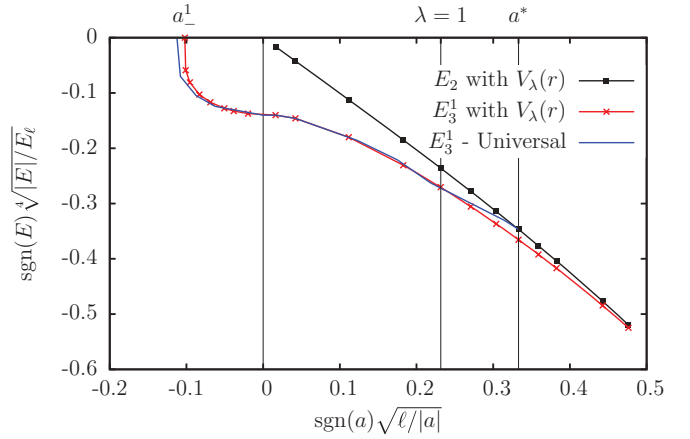
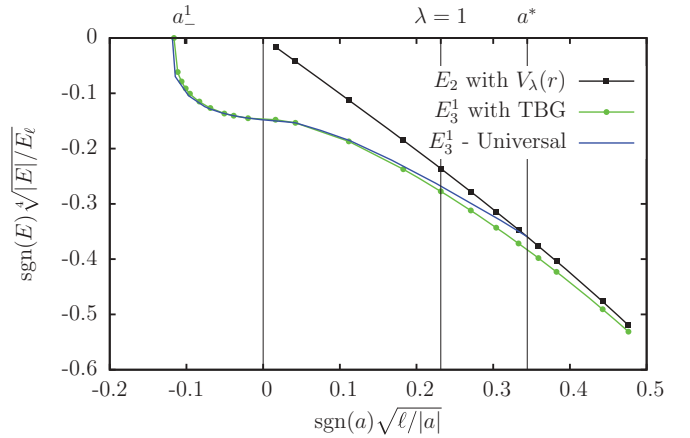


FIG. 5. (Color online) Comparison between the excited three-body energy E_3^1 and the theoretical universal value given by Eq. (4), using the TBG potential (upper panel) and the modified LM2M2 potential $V_\lambda(r)$ (lower panel). The two-body energy E_2 calculated with $V_\lambda(r)$ is also shown. The calculated and theoretical curves agree around the resonant limit, and the differences close to the values a^* and a_-^1 are due to effective-range corrections. The most remarkable difference is represented by the fact that the calculated E_3^1 does not cross the atom-dimer threshold.

$\Delta(-\pi/4) = 6.02730678199$ and $\Delta(-\pi) \approx -0.89$ [1], it is possible to determine the values a^* (at which $E_3^1 = E_2$) and a_-^1 (at which $E_3^1 = 0$). In order to analyze the universal character of the calculated energies E_3^1 using the TBG and TBG + H3B potential models, in Fig. 5 we compare them to the values of Eq. (4). By construction, the energies E_3^1 at the resonant limit coincide with those of Eq. (4). It is possible to see that the calculated energies using the TBG potential (Fig. 5 upper panel) and TBG + H3B potential (Fig. 5 lower panel) reproduce the universal behavior close to the resonant limit. The small differences observed at finite values of a , especially close to the critical values a^* and a_-^1 , are due to effective-range corrections which are automatically included in our approach. Moreover, E_3^1 does not disappear in the atom-dimer continuum at a^* , but follows very close the E_2 curve from below.

To conclude, we further analyze the universality looking at the correlations between the three-body ground and excited states, as has been proposed in Ref. [32]. In Fig. 6 we trace the square root of the excited-trimer energy, measured from

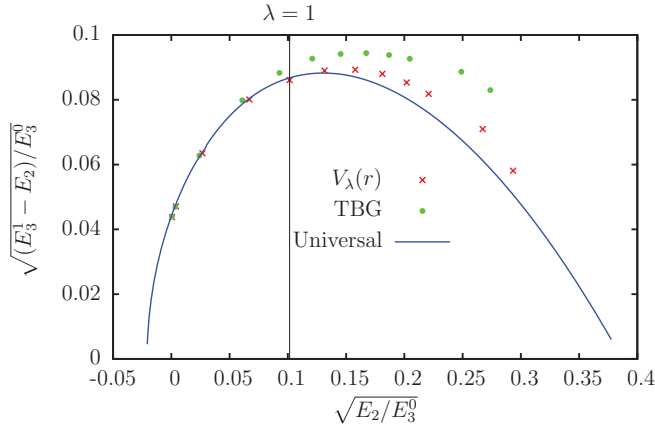


FIG. 6. (Color online) Correlations between the ground E_3^0 and excited E_3^1 states of the trimer. We compare the universal correlation, obtained by means of Eq. (4), to the calculations made using the full $V_\lambda(r)$ potential and the TBG potential. The agreement is good close to the unitary point, where the dimer energy E_2 is small. The deviations become significant when the finite effective-range effects become non-negligible.

the two-body dimer, in units of the trimer ground-state energy, as a function of the dimer energy, always in units of trimer ground-state energy. Efimov's universal-radial law [Eq. (4)] gives the universal curve in this plot; we see that as far as the dimer is very shallow, the calculated points are very close to the universal curve. They depart from it when corrections due both to finite scattering length and to nonzero effective range become sizable. This nonuniversal effect is more important for the TBG case, probably due to the lack of the three-body corrections.

IV. EFIMOV PLOT FOR $A = 4, 5, 6$ CLUSTERS

The calculations for the $A > 3$ systems are performed using the NSHH basis. The method has been recently used to describe up to six nucleons interacting through a central potential [21,22,33] and six bosons using a two-body plus a three-body force [17]. The Hamiltonian matrix is obtained using the following orthonormal basis:

$$\langle \rho \Omega | m [K] \rangle = \left(\beta^{(\alpha+1)/2} \sqrt{\frac{m!}{(\alpha+m)!}} L_m^{(\alpha)}(\beta\rho) e^{-\beta\rho/2} \right) \mathcal{Y}_{[K]}^{LM}(\Omega_N), \quad (5)$$

where $L_m^{(\alpha)}(\beta\rho)$ is a Laguerre polynomial with $\alpha = 3N - 1$ ($N = A - 1$) and β a variational nonlinear parameter. The functions $\mathcal{Y}_{[K]}^{LM}(\Omega_N)$ are the HH functions with grand angular momentum K , and total angular momenta L and magnetic number M . The Hamiltonian matrix is not constructed, but using properties of HH is expressed as an algebraic combination of sparse matrices, allowing for an efficient research of the lowest eigenvectors/eigenvalues. A full discussion of the NSHH method is given in Refs. [17,22].

After solving the $A = 3$ problem for bound states, used to fix the strength of the H3B force, we have diagonalized the Hamiltonian for $A = 4, 5, 6$ bodies using the TBG and TBG + H3B potentials. The results are given in Fig. 7 in two

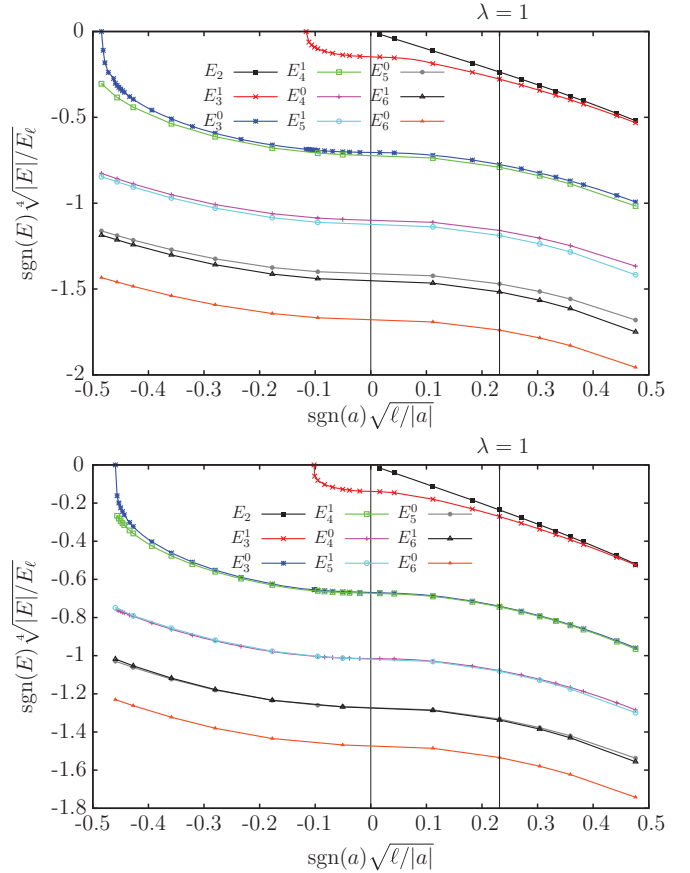


FIG. 7. (Color online) Energies of the $A = 3 - 6$ ground and excited states, E_A^0, E_A^1 , as a function of a^{-1} , using the two-body Gaussian potential (upper panel), and using the two-body plus the hypercentral three-body force (lower panel). In both panels, we also give the two-body ground-state energy E_2 calculated with the LM2M2 potential.

scaled (a^{-1}, κ) plots, one obtained with the two-body potential alone (upper panel) and one with the two-body plus three-body interactions (lower panel). In the first case, with only the TBG potential, we observe that the spectrum of the systems $A = 4, 5, 6$ presents two bound states, one deep and one shallow, for all values of a studied. When the repulsive three-body force is included, the spectrum moves up and we can observe that the excited state E_A^1 disappears for $A = 5, 6$ for negative values of the scattering length as a approaches a_-^1 . This fact is better shown in Fig. 8, where the differences $E_A^0 - E_{A+1}^1$ have been plotted as functions of ℓ/a . Whereas the differences $E_2^0 - E_3^1$ and $E_3^0 - E_4^1$ are positive along the whole range, indicating that the states E_3^1 and E_4^1 are bound, the differences $E_4^0 - E_5^1$ and $E_5^0 - E_6^1$ result negative as a goes to the negative region, so at some value of a the excited states E_5^1 and E_6^1 are no more bound. The determination of the point where the transition happens can be determined by looking at the convergence of the states E_5^1 and E_6^1 , as can be seen in Table II where we report the convergence pattern using the TBG + H3B potential for $A = 4, 5, 6$ at the point $\lambda = 0.9$ where both E_5^1 and E_6^1 are not bound. They remain above the E_4^0 and E_5^0 thresholds, respectively. In the table, we have shown the three maximum values of K considered in the present calculations.

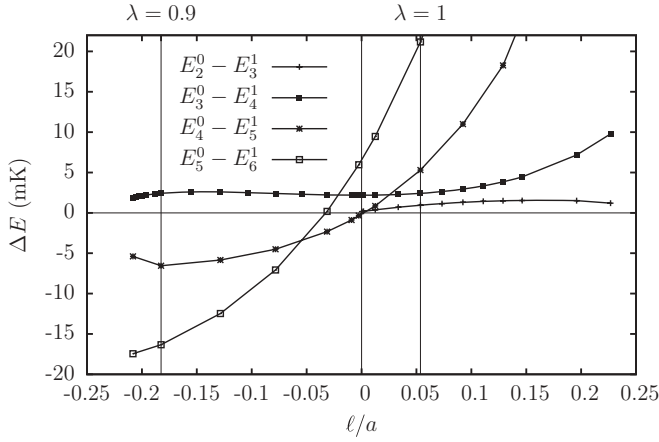


FIG. 8. The difference $\Delta E = E_A^0 - E_{A+1}^1$ for the indicated cases as a function of the inverse of a for the TBG + H3B potential. The particular cases at $\lambda = 1$ and 0.9 as well as at the unitary limit are indicated as vertical lines.

Moreover, the fact that the states E_5^1 and E_6^1 are bound or not depends also on the range of the three-body force ρ_0 . In order to analyze this relation, we have varied ρ_0 at $\lambda = 0.9$ as well as at the unitary limit. For each value of ρ_0 , the strength of the three-body potential has been fixed to reproduce the trimer binding energy E_3^0 as before. The results for $A = 4, 5, 6$ at $\lambda = 0.9$ are shown in Fig. 9. As can be seen, the excited states are recovered as bound states for values of $\rho_0 \approx 18$ a.u.

To make contact with the analysis of Ref. [34], we have calculated $\sqrt{|E_4^1 - E_3^0|/|E_4^0|} = 0.070$ and $\sqrt{|E_3^0|/|E_4^0|} = 0.434$ at the unitary limit. These two values correspond to a point in the plot given in Fig. 1 of that reference lying very close to the line giving the relation of these two quantities at the unitary limit. In addition, in Fig. 10 we analyze the relation between E_{A+1}^0 (upper panel) and E_{A+1}^1 (lower panel) with E_A^0 and E_A^1 , respectively, as a function of the scattering length for $A = 4, 5, 6$. We can observe a linear dependence in all cases except for a small curvature in the E_4^0 versus E_3^0 and E_4^1 versus E_3^1 curves close to the point in which E_3^0 goes to zero. These curves display the universal character of these clusters as their spectrum is determined by two parameters, a and E_3^0 .

TABLE II. Convergence of the binding energies as a function of the grand angular quantum number K using the TBG + H3B potential at $\lambda = 0.9$, $R_0 = 10$ a.u., and $\rho_0 = 10$ a.u. for clusters of A particles. We also report the number N_{HH} of hyperspherical basis elements corresponding to a given K .

A	K	N_{HH}	E_A^0 (mK)	E_A^1 (mK)
4	36	33649	-166.25945	-6.55041
	38	42504	-166.25949	-6.79163
	40	53130	-166.25951	-6.99574
5	26	448800	-532.75811	-161.96737
	28	724812	-532.75828	-162.98374
	30	1139544	-532.75834	-163.79689
6	18	709410	-1063.8276	-513.50956
	20	1628328	-1063.8311	-516.42712
	22	3527160	-1063.8322	-518.25341

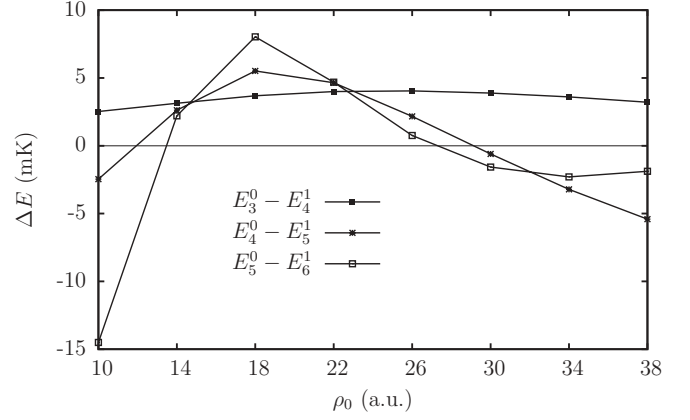


FIG. 9. The difference $\Delta E = E_A^0 - E_{A+1}^1$ at $\lambda = 0.9$ as a function of ρ_0 for the TBG + H3B potential.

Besides, the universal ratios E_A^0/E_3^0 and E_{A+1}^1/E_A^0 can be studied at $\lambda = 1$. They are $E_4^0/E_3^0 = 4.5$, $E_5^0/E_3^0 = 10.4$, $E_6^0/E_3^0 = 18.4$ and $E_4^1/E_3^0 = 1.020$, $E_5^1/E_4^0 = 1.009$, $E_6^1/E_5^0 = 1.016$. These ratios are in close agreement to those obtained in the literature [23]. At the unitary limit, the ratios E_A^0/E_3^0 move a little bit from the universal values showing some dependence on the form of the soft potential, whereas the ratios E_{A+1}^1/E_A^0 show stability. At $\lambda = 0.9743$,

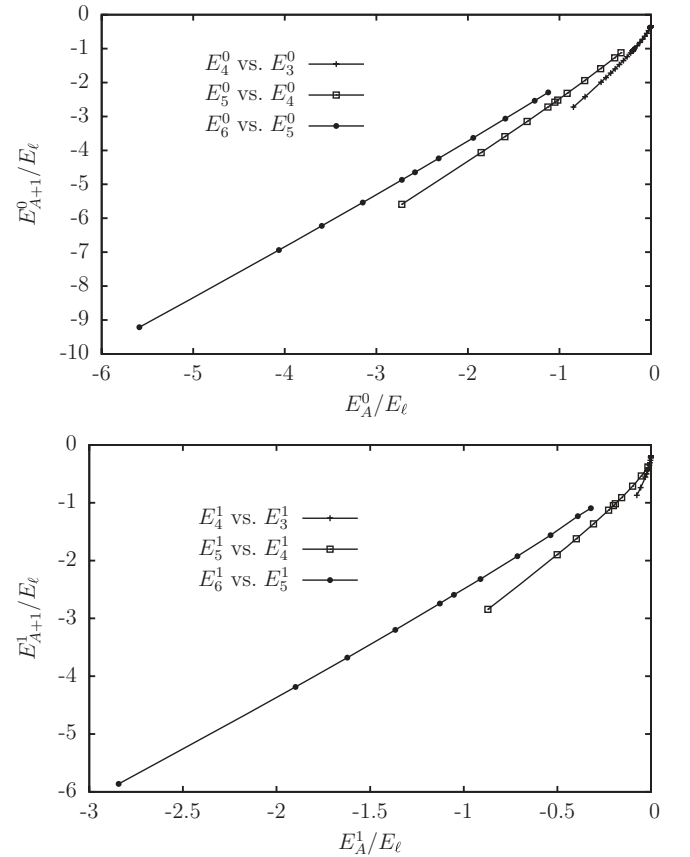


FIG. 10. Relation between E_{A+1}^0 and E_A^0 (upper panel) and between E_{A+1}^1 and E_A^1 (lower panel) for the indicated cases obtained with the TBG + H3B potential along the (a^{-1}, κ) plane.

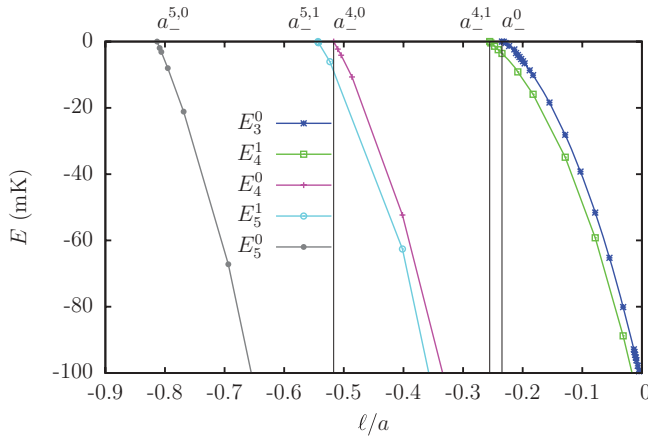


FIG. 11. (Color online) Energies of the states E_3^0 , E_4^1 , E_4^0 , E_5^1 , and E_5^0 as a function of a^{-1} for negative values of the scattering length close to the continuum threshold obtained using the TBG potential. The four-particle thresholds are $a_-^{4,0} \approx -19.6$ a.u. and $a_-^{4,1} \approx -39.8$ a.u. The five-particle thresholds are $a_-^{5,0} \approx -12.5$ a.u. and $a_-^{5,1} \approx -18.7$ a.u.

they are $E_4^0/E_3^0 = 5.3$, $E_5^0/E_3^0 = 13.0$, $E_6^0/E_3^0 = 23.4$ and $E_4^1/E_3^0 = 1.026$, $E_5^1/E_4^0 = 1.004$, $E_6^1/E_5^0 = 1.006$.

Finally, using the TBG potential, we have extended the calculations for $A = 4$ and 5 systems up to the four- and five-particle thresholds in order to calculate the ratios between the different thresholds and to compare our results to previous calculations and experimental outcomes. Our results are summarized in Fig. 11. Denoting with $a_-^{4,0}$ and $a_-^{4,1}$ the four-particle thresholds of the ground and excited states, respectively, we have $a_-^{4,1} \approx -39.8$ a.u., and $a_-^{4,0} \approx -19.6$ a.u.; equivalently, with respect to the three-particle threshold a_-^0 we get $(a_-^{4,1}/a_-^0)_{\text{TBG}} \approx 0.92$ for the excited state, and $(a_-^{4,0}/a_-^0)_{\text{TBG}} \approx 0.45$ for the ground states. These values agree very well with what was measured in the experiments [24–26] and with what was predicted by the theory [7,23,35]. The five-particle thresholds read as $a_-^{5,0} \approx -12.5$ a.u. for the ground state and $a_-^{5,1} \approx -18.7$ a.u. for the excited state. Equivalently, the ratios with respect to the four-particle threshold are $(a_-^{5,0}/a_-^{4,0})_{\text{TBG}} \approx 0.64$ and $(a_-^{5,1}/a_-^{4,0})_{\text{TBG}} \approx 0.95$, still in agreement with previous theoretical prediction [23] and with recent experiments [27].

V. CONCLUSIONS

In this paper, we have discussed the spectrum of bosonic systems up to six particles interacting through a two-body potential having a large two-body scattering length (with respect to the effective range). The three-body scale has been fixed using a scaled helium-helium potential. The scope was to extend previous studies on the Efimov physics done in the three- and four-body systems. We have observed that, similarly to the four-body system, the five- and six-body systems present two bound states, one deep and one shallow. It seems that this type of spectrum is to some extent universal depending only on the condition $a \gg r_0$ in the two-body system. This condition produces a geometrical series of bound states in the three-body system and, attached to each of these states, a

two-level spectrum has been showed to appear in the four-body system [6–8]. However, they are true bound states only in correspondence to the lowest trimer level. The other states appear as resonances embedded in the continuum of four particles. It is possible to introduce a repulsive three-body force that eliminates all the trimer states below one specific level. In this way, the two-level spectrum of the four-body system attached to this trimer ground state will become true bound states. Also, the universal character of the spectrum will be more evident as the repulsive three-body force will push more and more the particles far away.

Although the analysis of the bosonic spectrum can follow the strategy illustrated above, in this paper we follow a different one based on the physics introduced by the two-body potential. In nuclear systems as well as in many atomic systems, the two-body interaction has a sharp repulsion at short range followed by a very weak attractive part that produces very shallow dimers as, for example, the deuteron or the two-helium molecule. The particles are located in the asymptotic region and do not feel the details of the interaction. Therefore, we can introduce a soft potential to be considered as a regularized two-body contact term in an EFT approximation of the original potential [19]. In the three-body sector, a three-body contact term is required to reproduce the ground-state binding energy of three particles introduced here by means of a Gaussian-hypercentral three-body force. Using this potential model, we have calculated the three-body spectrum and we have analyzed its universal character comparing the energy of the shallow state E_3^1 to Efimov's equation for the binding energy. Furthermore, we have identified the critical values a_-^0 and a_-^1 at which $E_3^0 = 0$ and $E_3^1 = 0$, respectively. Successively, we have calculated the four-, five-, and six-body spectra and we have observed the two-level structure. The EFT approach is better adapted to describe shallow states and this is confirmed by the close result obtained for $E_4^1 = -128.8$ mK at $\lambda = 1$ and the LM2M2 result $E_4^1 = -127.9$ mK, very recently published [14].

The universal character of the structure of these clusters has been studied using Tjon lines, which means the relation between E_{A+1}^0 and E_A^0 and between E_{A+1}^1 and E_A^1 . As illustrated in Fig. 10, we have obtained an almost linear relation between E_{A+1}^0 and E_A^0 (upper panel) and between E_{A+1}^1 and E_A^1 (lower panel) in the region from $\lambda = 1$ to 0.9 . As the energy of the cluster E_A^0 or E_A^1 tends to zero, the linear relation is lost.

Since we are describing the lowest bound states, some universal ratios are only approximately verified, although not very far from the values quoted by other groups in $A = 3, 4$. However, in the simple case of TBG, we have extended our calculations for $A = 4$ and 5 up to the four- and five-particle continuum threshold in order to calculate the ratios between the thresholds: the values we obtain in the four-body case $(a_-^{4,1}/a_-^0)_{\text{TBG}} \approx 0.92$ and $(a_-^{4,0}/a_-^0)_{\text{TBG}} \approx 0.45$, and in the five-body system $(a_-^{5,0}/a_-^{4,0})_{\text{TBG}} \approx 0.64$ and $(a_-^{5,1}/a_-^{4,0})_{\text{TBG}} \approx 0.95$, are in accord with the ratios that have been previously predicted [36] and measured [27] in literature.

Another interesting aspect is the uncertainty introduced by the cutoff in the hypercentral three-body force. We have observed that with the most natural choice $\rho_0 = R$, the shallow

states E_5^1 and E_6^1 result unbound in the last part of the curves. They cross the respective thresholds E_4^0 and E_5^0 . Increasing ρ_0 , they result bound again around $\rho_0 \approx 18$ a.u. Increasing further ρ_0 , they become again unbound. This last analysis is somehow inconclusive as to really understand the cutoff dependence we need to vary both cutoff R_0 and ρ_0 in a

coherent way; the dependence on the cutoff will eventually reflect the leading-order nature of the potential we are using, pointing to the necessity of going to a higher order in the EFT expansion [19]. Studies along this line are at present under consideration as well as the analysis of the two-level spectrum for cluster with more than six particles.

-
- [1] E. Braaten and H. Hammer, *Phys. Rep.* **428**, 259 (2006).
- [2] C. H. Greene, *Phys. Today* **63**(3), 40 (2010).
- [3] F. Ferlaino and R. Grimm, *Physics* **3**, 9 (2010).
- [4] V. Efimov, *Phys. Lett. B* **33**, 563 (1970).
- [5] V. Efimov, *Sov. J. Nucl. Phys.* **12**, 589 (1971) [*Yad. Fiz.* **12**, 1080 (1970)].
- [6] L. Platter, H. W. Hammer, and Ulf-G. Meissner, *Phys. Rev. A* **70**, 052101 (2004).
- [7] J. von Stecher, J. P. D’Incao, and C. H. Greene, *Nat. Phys.* **5**, 417 (2009).
- [8] A. Deltuva, R. Lazauskas, and L. Platter, *Few-Body Syst.* **51**, 235 (2011).
- [9] H. W. Hammer and L. Platter, *Eur. Phys. J. A* **32**, 113 (2007).
- [10] E. A. Kolganova, A. K. Motovilov, and S. A. Sofianos, *J. Phys. B: At., Mol. Opt. Phys.* **31**, 1279 (1998).
- [11] E. Nielsen, D. V. Fedorov, A. S. Jensen, and E. Garrido, *Phys. Rep.* **347**, 373 (2001).
- [12] P. Barletta and A. Kievsky, *Phys. Rev. A* **64**, 042514 (2001).
- [13] M. Lewerenz, *J. Chem. Phys.* **106**, 4596 (1997).
- [14] E. Hiyama and M. Kamimura, *Phys. Rev. A* **85**, 022502 (2012).
- [15] N. K. Timofeyuk, *Phys. Rev. C* **78**, 054314 (2008).
- [16] A. Kievsky, E. Garrido, C. Romero-Redondo, and P. Barletta, *Few-Body Syst.* **51**, 259 (2011).
- [17] M. Gattobigio, A. Kievsky, and M. Viviani, *Phys. Rev. A* **84**, 052503 (2011).
- [18] R. A. Aziz and M. J. Slaman, *J. Chem. Phys.* **94**, 8047 (1991).
- [19] P. Lepage, in *Nuclear Physics: Proceedings of the VIII Jorge André Swieca Summer School, 1995*, edited by C. A. Bertulani *et al.* (World Scientific, Singapore, 1997), p. 135.
- [20] M. Gattobigio, A. Kievsky, M. Viviani, and P. Barletta, *Phys. Rev. A* **79**, 032513 (2009).
- [21] M. Gattobigio, A. Kievsky, M. Viviani, and P. Barletta, *Few-Body Syst.* **45**, 127 (2009).
- [22] M. Gattobigio, A. Kievsky, and M. Viviani, *Phys. Rev. C* **83**, 024001 (2011).
- [23] J. von Stecher, *J. Phys. B: At., Mol. Opt. Phys.* **43**, 101002 (2010).
- [24] S. E. Pollack, D. Dries, and R. G. Hulet, *Science* **326**, 1683 (2009).
- [25] M. Zaccanti, B. Deissler, C. D’Errico, M. Fattori, M. Jonas-Lasinio, S. Müller, G. Roati, M. Inguscio, and G. Modugno, *Nat. Phys.* **5**, 586 (2009).
- [26] F. Ferlaino, S. Knoop, M. Berninger, W. Harm, J. P. D’Incao, H. C. Nägerl, and R. Grimm, *Phys. Rev. Lett.* **102**, 140401 (2009).
- [27] A. Zenesini, B. Huang, M. Berninger, S. Besler, H. C. Nägerl, F. Ferlaino, R. Grimm, C. H. Greene, and J. von Stecher, arXiv:1205.1921.
- [28] B. D. Esry, C. D. Lin, and C. H. Greene, *Phys. Rev. A* **54**, 394 (1996).
- [29] A. Kievsky, L. E. Marcucci, S. Rosati, and M. Viviani, *Few-Body Syst.* **22**, 1 (1997).
- [30] P. Naidon, E. Hiyama, and M. Ueda, *Phys. Rev. A* **86**, 012502 (2012).
- [31] M. Berninger, A. Zenesini, B. Huang, W. Harm, H. C. Nägerl, F. Ferlaino, R. Grimm, P. S. Julienne, and J. M. Hutson, *Phys. Rev. Lett.* **107**, 120401 (2011).
- [32] T. Frederico, L. Tomio, A. Delfino, and A. E. A. Amorim, *Phys. Rev. A* **60**, R9 (1999).
- [33] M. Gattobigio, A. Kievsky, and M. Viviani, *J. Phys.: Conf. Ser.* **336**, 012006 (2011).
- [34] M. R. Hadizadeh, M. T. Yamashita, L. Tomio, A. Delfino, and T. Frederico, *Phys. Rev. Lett.* **107**, 135304 (2011).
- [35] A. Deltuva, arXiv:1202.0167.
- [36] J. von Stecher, *Phys. Rev. Lett.* **107**, 200402 (2011).